Hearing-Aid Compatibility Focused Near-Field Control of Handset Antennas Based on Inverted-Top Wavetraps

Jabez Daniel.V.D.M
Assistant Professor/ECE, Dr.Sivanthi Aditanar College of Engineering, Tiruchendur

Abstract

In this letter, it is shown that inverted-top wavetraps, which are quarter-wavelength-long resonators, can be used to con-trol the near-fields of a mobile terminal antenna. The local reduc-tion of the near-fields is especially important for the operation of the hearing aid of the user. The reshaping of the near-fields may also enable reduced specific absorption rate (SAR) values.

Index Terms - *Electromagnetic compatibility (EMC), electro-magnetic interference, hearing aids, microstrip antennas, mobile antennas.*

I. INTRODUCTION

A HEARING AID is an electro acoustic apparatus that is typically placed in or behind the user's ear and is designed to amplify and modulate sounds for the user. A mobile terminal used beside the user's ear may cause electromagnetic compati-bility (EMC) problems on the hearing-aid operation, especially due to the near-fields of the antennas. This issue has been recog-nized, e.g., in the USA, where a standard for the compatibility of hearing aids and mobile terminals was introduced [1], and obviously the standard will get more widely introduced around the world in the near future. From the terminal manufacturers' point of view, the standard is in the first place related to the cel-lular antennas that create the near-fields. To fulfill the current hearing-aid compatibility (HAC) standard with traditional an-tenna solutions without sacrificing the far-field radiation prop-erties is not a trivial task. According to the authors' knowledge, there exist not many published antenna structures satisfying the HAC standard. One antenna solution is introduced in [2]. In this letter, another solution is proposed.

II. HEARING - AID COMPATIBILITY STANDARD

The standardized method of measuring the HAC [1] defines the tests to be done in free-space (without the user) on a square HAC plane (base 50 mm) at a 15-mm distance from the surface of the phone. The center of the square plane is aligned with the earpiece of the mobile device. In this work, the earpiece is de-termined to be located at a 10-mm distance from the edge of the chassis of the terminal; see Fig. 1. Furthermore, the HAC plane is divided into nine equal-sized subgrids. For each sub-grid, the maximum of the electric and magnetic fields is mea-sured. According to the standard, three adjacent subgrids (ex-cept the center subgrid) can be excluded for both electric and magnetic fields so that one of the excluded subgrids has to be the same for both electric and magnetic fields. In the remaining six subgrids, the electric and magnetic field strengths have to be below the given limits in order to fulfill the HAC standard. The maximum field limits for the HAC standard M3 (articulation weighting factor ΛWF=−5 dB for GSM systems) are

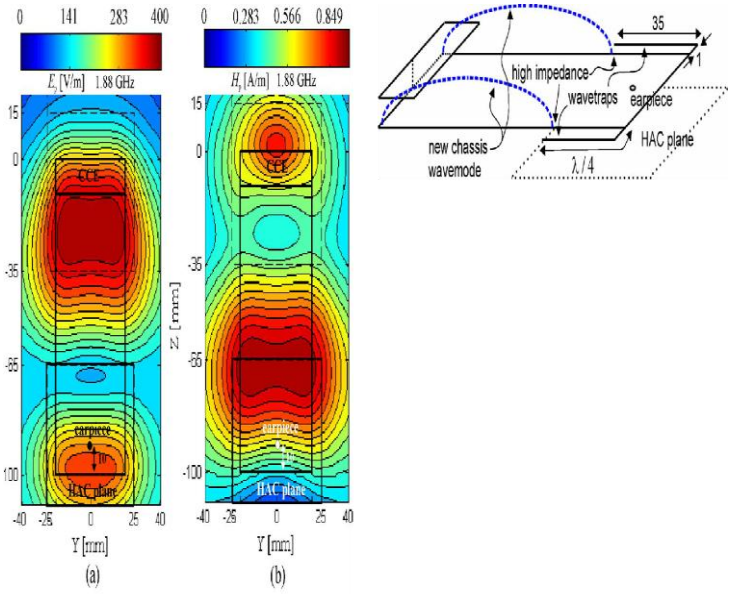

Fig. 2. (a) Electric and (b) magnetic fields on the HAC plane distance at 1.88 GHz for the full-metal antenna structure presented in Fig. 1

shown in Table I. As can be seen, the standard field values are much stricter above 0.96 GHz. Thus, it is assumed that it is more difficult to fulfill the standard at the upper GSM frequencies.

III. INVERTED-TOP WAVETRAPS

A. Chassis Radiation and Wavemodes

As it is well known, the chassis of a mobile terminal has a significant effect on the antenna operation because the chassis operates as a significant radiator below 2 GHz [3]. The chassis supports a thick dipole-type current distribution and has certain resonant wavemodes [3]. The first-order wavemode exists when the chassis is electrically half-wavelength long; see Fig. 1. The second resonance is reached with an electrically wavelength-long chassis. At the existing GSM frequencies, the current distribution of the chassis is the superposition of the two lowest order wavemodes. In this letter, the chassis wavemodes are excited with bottom-located capacitive cou-pling elements (CCEs) introduced in [4]. The two lowest order wavemodes of the chassis introduce the zero of the electrical current in the open-end of t

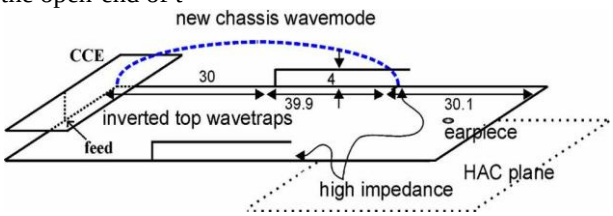

Fig. 3. Idea of quarter-wavelength-long wavetraps.
Fig. 4. Idea of inverted-top wavetraps.

the chassis; see Fig. 1. In the case of standing waves, the voltage (or the electric field) maxima occur at the same place as the current minima (or zeros). Thus, in the vicinity of the open-end of the chassis—i.e., on the HAC plane—there exist strong electric fields. The electric and magnetic fields of the antenna structure in Fig. 1 are simulated on the HAC plane distance (15 mm) with SEMCAD X elec-tromagnetic simulator [5]. The fields are shown at the center frequency of the GSM1900 transmission band (1.88 GHz). The results are normalized to the maximum transmitted power (1 W) of the system, and the peak field values are shown in Fig. 2. As can be seen, the simulated electric field values for this fairly ideal full-metal design are high and actually not even close to the limits of the specifications given in Table I.

B. Idea of Inverted-Top Wavetraps

In order to affect the near-fields of the antenna on the HAC plane, the electric current distribution of the chassis needs to be somehow reshaped. That can be done, e.g., by using wave-traps introduced in [6]; see Fig. 3. The wavetraps operate in a similar way as a balun, in which a high-impedance location is created with a short-circuited, quarter-wavelength-long trans-mission line. One can then create a high-impedance location on the chassis and thus create a new chassis wavemode and espe-cially avoid the zero of the electric currents in the open-end of the chassis. In [6], an enhancement of the impedance bandwidth was demonstrated with the wavetraps. In [7], the wavetraps have been used to increase the radiation efficiency of a handset an-tenna for certain users' hand grips. In Fig. 3, the wavetraps are quarter-wavelength long at 1.88 GHz. At the frequencies of GSM850, the wavetraps as such would be unfeasibly long, and hence, this letter concentrates only on the upper GSM band. The field distributions are not shown, but the wavetraps can re-duce the electric fields on the HAC plane compared to the case without the wavetraps. However, these kinds of wavetraps do not limit the magnetic fields on the HAC plane since the strong electric currents in the wavetraps locally create very high mag-netic fields.

In order to avoid strong local electric and magnetic fields on the HAC plane, we introduce *inverted-top wavetraps*. They are based on the same principle of creating a high-impedance envi-ronment at certain locations on the ground plane as the wave-traps presented above, but the orientation of the inverted-top wavetraps is different, as can be seen in Fig. 4. The lowest field strengths on the HAC plane are achieved when the inverted wavetraps are located on the top of the chassis rather than on the sides—hence, inverted-*top* wavetraps. The dimensions of the in-verted-top wavetraps in Fig. 4 are optimized in such a way that the quarter-wavelength resonance of the wavetrap is achieved at 1.88 GHz. In addition, the distance of the wavetraps from the antenna-element end of the chassis is optimized so that the resonant frequency of the new wavemode of the chassis is also 1.88 GHz. This is very useful because the impedance bandwidth maxima of the antenna are achieved at the resonant wavemode frequencies of the chassis [3]. In addition, the location of the inverted-top wavetraps is far enough from the HAC plane.

The near-fields of the structure in Fig. 4 are presented in Fig. 5. As can be seen, both electric and magnetic fields can be reduced on the HAC plane with the help of the inverted-top wavetraps. Compared to the case without the wavetraps, both field values are decreased up to 74% at 1.88 GHz.

However, one should note that the maximum decrease of the fields on the HAC plane is achieved only at the quarter-wave-length resonant frequency of the wavetraps. However, with the simulations it was found that within the GSM1900 TX band (1.85–1.91 GHz), the electric and magnetic fields compared to the lowest field values achieved at 1.88 GHz increase only 43% and 32%, respectively—i.e., less than 3 dB. Hence, compared to the case without the wavetraps, the electric and magnetic field

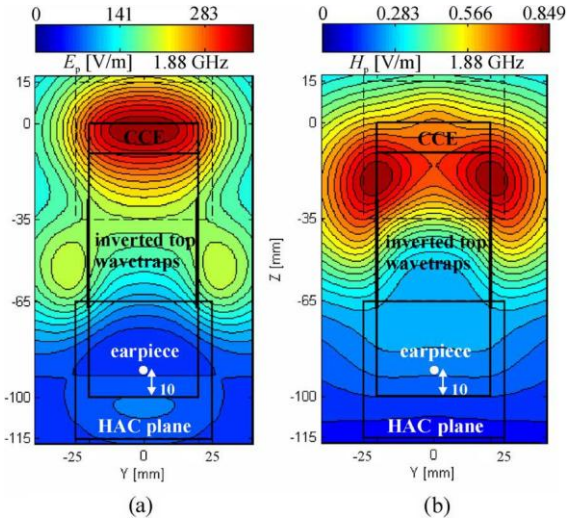

Fig. 5. (a) Electric and (b) magnetic fields on the HAC plane of the full-metal antenna structure presented in Fig. 4.

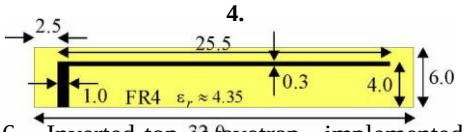

Fig. 6. Inverted-top wavetrap implemented with stripline on a piece of 1-mm-thick FR4. The black strips are metallic, and the shading depicts the substrate of FR4. The reverse side of FR4 is nonmetallic.

values are decreased up to 63% and 66%, respectively, within the GSM1900 TX band. The near-field values across the TX band may be further decreased by using multiresonant wavetraps consisting, e.g., of multi-branch structures.

The specific absorption rate (SAR) of the antenna at 1.88 GHz was also simulated at a 4-mm distance from the SAM head model. The 1-g average maximum SAR is 0.64 W/kg with 0.125-W input power. When comparing to the reference without the wavetraps, the SAR value is decreased 23% by the wavetraps. This happens because the wavetraps direct the near-fields away from the head.

IV. PROTOTYPE

A prototype based on the antenna structure shown in Fig. 4 was designed, manufactured, and measured. The inverted-top wavetraps are implemented on a piece of 1-mm-thick FR4 sub-strate. The wavetraps are shown in Fig. 6, and the photograph of the prototype is shown in Fig. 7.

A. Measured Return Loss

The antenna was matched with a matching circuit consisting of a 1.6-pF parallel capacitor (from Murata GQM18 series). The measured return loss is shown in Fig. 8. Due to the new chassis wavemode created by the wavetraps, the dual-resonant opera-tion makes it possible to cover 17% relative bandwidth with 6-dB return loss. The wavetraps used here enhance the band-width the same way as presented in [6]. By further optimizing the matching circuit, it would be possible to cover GSM1800/ 1900 and UMTS systems.

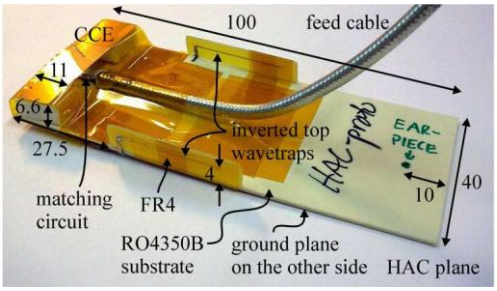

Fig. 7. Photograph of the prototype. The dimensions are in millimeters.

B. Near Fields

Next, the near-fields were measured with DASY4 measure-ment system [8]. To be able to normalize the field values to 1-W radiated power, the total efficiency of the prototype was measured with Satimo Stargate measurement system. The total efficiency is needed to ensure that the prototype is radiating efficiently enough and the reduction of the near-fields is not achieved at the expense of the total efficiency. The measured total efficiencies are 0.53, 0.66, and 0.61 at 1.85, 1.88, and 1.91 GHz, respectively. The smallest fields were achieved at the lowest edge of the GSM1900 TX band—i.e., at 1.85 GHz—in-stead of the design frequency of 1.88 GHz. This down-tuning in frequency is obviously happening because the wavetraps were implemented on the FR4 substrate, for which the relative permittivity may differ from the given nominal value, and therefore, the resonant frequency of thewavetraps is slightly tuned down from the desired 1.88 GHz. The measured fields at 1.85 GHz are illustrated in Fig. 9. Slight asymmetry in the field distributions is due to the fact that one of the wavetraps was slightly slanted due to the mechanical reasons.

In order to have fair comparison between the simulated and measured results, in the simulations, the wavetraps are quarter-wavelength long at 1.85 GHz. The simulated field distributions are shown in Fig. 10. The simulated and measured maximum values agree pretty well. The difference in the results is obvi-ously due to the fairly ideal simulation model and the measure-ment inaccuracy. At 1.88 GHz, the measured maximum electric and magnetic field values after the exclusion are 104 V/m and 0.28 A/m, respectively, and at 1.91 GHz, 137 V/m and 0.37 A/m.

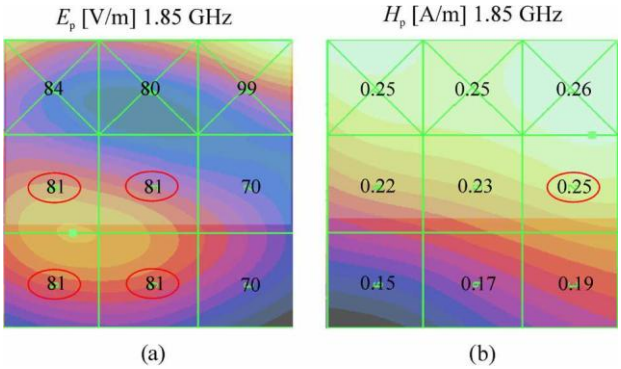

Fig. 9. Measured (a) electric and (b) magnetic fields of the prototype on the HAC plane (peak values) with the allowed exclusions according to the HAC standard.

Table II Summary Of The Field Values Of The Prototype

Peak field values	HAC specification field limits	Prototype simulated 1.85 GHz	Prototype measured 1.85 GHz	Reference measured 1.85 GHz
Electric [V/m]	< 84.1	92.2	81	290
Magnetic [A/m]	< 0.25	0.255	0.25	0.77

V. CONCLUSIONS

In this letter, it was shown with simulations and measure-ments that the inverted-top wavetraps used with bottom-located antenna elements can reduce the electric and magnetic fields of the GMS1900 system antenna on the hearing-aid compat-ibility plane. The use of the inverted-top wavetraps is limited only to bottom-located antenna elements, but not only to capac-itive coupling elements. Therefore, it was tested with simula-tions that the wavetraps work effectively also with (bottom-lo-cated) traditional antenna elements, such as planar inverted-F antennas (PIFAs). Since the inverted-top wavetraps are based on the quarter-wavelength resonance, the best hearing-aid com-patibility performance is achieved at the resonant frequency of the wavetraps. However, multiresonant wavetraps may increase the operation bandwidth of the wavetraps. It was tested with the simulations that the antennas of other systems are not af-fected by the wavetraps. It was also shown that it is possible to decrease the specific absorption rate using the inverted-top wavetraps. The future outlook of the inverted-top wavetrap idea includes studies on the effect of the battery, display, and other relevant parts of a real handset on the near-fields. Preliminary results propose that the operation of the wavetraps is also pos-sible in the vicinity of the battery and/or other metallic parts.

REFERENCES

[1] American National Standard for Method of Measurements of Compat-ibility Between Wireless Communication Devices and Hearing Aids, ANSI C63.19-2007, Amer. Nat. Standards Inst., New York, 2007.

[2] T. Yang, W. A. Davis, W. L. Stutzman, and M.-C. Huynh, "Cellular-Phone and hearing-aid interaction: An antenna solution," IEEE An-tennas Propag. Mag., vol. 50, no. 3, pp. 51–65, Jun. 2008.

[3] P. Vainikainen, J. Ollikainen, O. Kivekäs, and I. Kelander, "Res-onator-Based analysis of the combination of mobile handset antenna and chassis," IEEE Trans. Antennas Propag., vol. 50, no. 10, pp. 1433–1444, Oct. 2002.

[4] J. Villanen, J. Ollikainen, O. Kivekäs, and P. Vainikainen, "Coupling element based mobile terminal antenna structures," IEEE Trans. An-tennas Propag., vol. 54, no. 7, pp. 2142–2153, Jul. 2007.

[5] SEMCAD X, a FDTD-based electromagnetic simulator ver. 13.4 Bernina, Schmid & Partner Eng. AG, Zurich, Switzerland, 2009 [Online]. Available: http://www.semcad.com/simulation/index.php

[6] P. Lindberg and E. Öjefors, "A bandwidth enhancement technique for mobile handset antennas using wavetraps," IEEE Trans. Antennas Propag., vol. 54, no. 8, pp. 2226–2233, Aug. 2006.

[7] Y. Okada, M. Yamamoto, and T. Nojima, "Unbalanced Fed Dipole Antenna Mounted on Ground Plane with L-shaped Parasitic Elements for Mobile Handsets," in Proc. ISAP 2008 Int. Symp. Antennas Propag., Taipei, Taiwan, Oct. 27–30, 2008, paper 1645395.pdf.